

On-line State of Charge Estimation of Embedded Metal Hydride Hydrogen Storage tank based on State Classification

Dan.Zhu^{a,b,*}, Youcef.Ait-Amirat^b, Abdoul.N'Diaye^b, Abdesslem.Djerdir^b

*^aSchool of Automobile, Chang'an University
Xi'an 710064, Shaanxi Province, China*

*^bFEMTO-ST, CNRS, Univ. Bourgogne Franche-Comte, UTBM
FCLAB, CNRS, Univ. Bourgogne Franche-Comte
Rue Thierry Mieg, F-90010 Belfort Cedex, France*

Abstract

With the further deterioration of environment and the depletion of fossil fuels, the alternative energy sources are urgently needed to be discovered. Hydrogen holds great promise thanks to its unlimited resources, high energy density and the environmentally friendly nature. However, its low volume density under normal temperature and pressure becomes the main challenge for on-board storage. Owing to its high potential of safety, one of the optimal solution for the future hydrogen vehicle is storing hydrogen using metal hydride (MH) under proper temperature and pressure. This work focuses on the state of charge (SOC) estimation of the embedded MH hydrogen storage tank. High precise estimating of the remaining energy will contribute to both the evaluation of reliability and the design of control strategy. A statistical model of SOC is proposed based on the database collected from laboratory experiments and real operation vehicle test. What's more, a joint multi-classifier is designed to recognize the current state of reaction. Under this condition, the SOC of MH hydrogen storage tank is calculated through combining the state classifier and SOC model. This proposed on-line SOC estimation procedure is validated with the real operation vehicles in both charging and discharging process. It is proved to be effective

*Corresponding author
Email address: dan.zhu@chd.edu.cn (Dan.Zhu)

with the estimation error of 0.2% during charging and 4.29% of discharging.

Keywords: Metal hydride, Hydrogen storage, On-line SOC estimation, State classification

1. Introduction

Hydrogen, produced from renewable energy, is being evaluated and promoted worldwide as an ideal power source for its inexhaustibility, cleanliness, convenience and independence from foreign control, which make it as the replacement for gasoline, heating oil, natural gas, and other fuels in both transportation and non-transportation applications [1, 2, 3]. For hydrogen vehicles, on-board hydrogen storage is one of the main challenges due to its low energy density per unit volume. Currently, hydrogen storage technologies including compressed hydrogen, liquefied hydrogen and hydrides, among them hydrogen storage in reversible metal hydrides (MH) has received great attention as it offers the possibility to store hydrogen at low pressure and moderate temperature with high volumetric density [4].

Hydride storage is material-based storage that hydrogen is physical or chemical absorbed reversibly by solid compounds under certain temperature and pressure conditions. During chemical sorption, chemical reaction occurs between hydrogen and material that hydrogen molecules are split into atoms and integrated with the storage material then generates hydride. The common used low temperature hydrides for hydrogen storage can be grouped based on the stoichiometries as AB_5 -type (e.g. $LaNi_5$), AB_2 -type (e.g. $Ti - Zr$ alloys), A_2B -type (e.g. Sb_2Ti , Sn_2Co) and AB -type (e.g. $Ti - Fe$ alloys), where A represents elements with high affinity for hydrogen typically rare-earth or alkaline earth metal (e.g., Ca , Ti , Zr , etc.) and B represents elements with low affinity for hydrogen typically a transition metal that forms only unstable hydrides (e.g., Cr , Mn , Fe , etc.) [5]. The quantities of hydrogen stored using metal hydride are quite large that the reaching volumetric density often higher than that of liquid hydrogen [6]. Besides, it holds potential benefits of security

27 compared to compressed hydrogen storage tank [7]. Although the compressed
 28 and low temperature liquid hydrogen storage tanks have already been widely
 29 used on commercial vehicles while the application of metal hydrides hydrogen is
 30 limited by the cost and weight for the current stage, storing hydrogen with MHs
 31 is still a promising method for embed hydrogen storing on the future hydrogen
 32 vehicle thanks to its high potential of density, safe and reliable.

33 State of charge (SOC) estimation is always an important issue and great
 34 challenge for all the energy storage device like battery, super-capacitor, oil tank
 35 and gas tank. Monitoring the remaining energy like electric, oil or nature gas
 36 in the device precisely is quite important for the energy management strategy
 37 design and the vehicle power train reliability evaluation [8]. Moreover, an ac-
 38 curate and efficient SOC estimation result reflects the health condition of the
 39 real applied energy storage device, which have a great impact on the control
 40 for practical operation in both charging and discharging process. Similarly, the
 41 SOC of a MH hydrogen storage tank should also be estimated to evaluate the
 42 remaining useful hydrogen. Especially for the design of an on-line SOC estima-
 43 tion method, from which the information of hydrogen mass storing in the tank
 44 is of great importance for the practical automobile application.

Generally, the hydrogen content of a MH sample is indicated by the hydrogen
 to host atomic ratio that:

$$r = \frac{H}{X} = \frac{n_H}{n_X} = \frac{m_H/M_H}{m_X/M_{MH}} \quad (1)$$

45 in which r represents the host atomic ratio, H and X indicate hydrogen and the
 46 host material separately. In this equation, n_H and n_X are the molar number
 47 of the hydrogen absorbed in the MH sample and the host material respectively.
 48 m_H and m_X are the mass of the hydrogen absorbed in the MH sample and
 49 the host material respectively. M_H is the molar mass of hydrogen and M_X
 50 represents that of host material. As to an energy storage device, the SOC at
 51 each sampling time i is the percentage of the remaining energy $m(i)$ to the total

Table 1 - List of symbols

Nomenclature	
MH	Metal hydride
SOC	State of Charge (%)
SVM	Support Vector Machine
NB	Naive Bayes
FCHEV	Fuel cell hybrid electrical vehicle
P-C-T	Pressure-Composition-Temperature
M_H	Molecular weight of hydrogen (g/mol)
M_{MH}	Molecular weight of one kind of MH (g/mol)
<i>Subscripts</i>	
<i>ini</i>	Initial State of the MH tank
<i>end</i>	Final state of the MH tank

52 amount of m_{total} , which can be written like the follow equation:

$$SOC(i) = \frac{m(i)}{m_{total}} * 100\% \quad (2)$$

53

54 From literature works, researchers proposed several methods for investigat-
55 ing the hydrogenation properties of a solid hydrogen storage sample. A number
56 of techniques are available to measure the hydrogen sorption capacity of a solid
57 reactor including the measurements of hydrogen pressure, component volume,
58 hydrogen flow and sample mass in a sample chamber, connected to a hydrogen
59 source, a hydrogen sink and a gas manifold [9]. One can also quote the Sievert
60 technique using the variation of pressure in a constant and calibrated system
61 volume to determine the hydrogen storage capacity [10]. It's well known for
62 the advantages of cost-effective, easy to set up, simple, physically robust and
63 reasonably reliable. However, researchers found it critically dependent on the
64 accurate volume calibration, especially for the high pressure measurement [11].
65 Gravimetric method is a reliable tool to measure the absorbed hydrogen mass

66 at high pressure condition, which determines the hydrogen sorption isotherm at
67 equilibrium state via mass measurement [12]. Secondary ion mass spectrometry
68 and neutron scattering are techniques based on the chemical composition
69 and physical structure analysis of the hydrogen storage materials. Using these
70 method, except for the accurate hydrogen capacity measurement, detailed in-
71 formation of hydrogenating reaction can be achieved and wider scale of material
72 can be tested [13, 14, 15]. Nevertheless, strict experimental conditions and ex-
73 pensive equipment make it confined to the sample analysis in laboratory. These
74 techniques are effective for the characterization of hydrogen and SOC estimation
75 of hydrogen storage materials while it is not suitable for practical application
76 of a hydrogen reactor, especially for the on-board hydrogen storage tanks in
77 transportation applications. For these applications of a MH hydrogen storage
78 reactor, the required SOC estimation method should be efficient, reversible and
79 movable.

80 Designing and simulating of the mathematical model is also an effective
81 method to observe the MH state variation during absorption or desorption pro-
82 cess [16]. Meanwhile, the relationship of the different effective factors like trans-
83 port properties, equilibrium situations and reaction kinetics can be determined
84 by the coefficients and functions [17, 18]. Researchers have proposed some MH
85 tank models to describe the reaction process. The first two-dimensional nu-
86 merical model is proposed by A. Jemni et al to emphasize the effect of the
87 shape, pressure and cooling system [19]. What's more, the three-dimensional
88 model figured out the parameters could be optimized to get an optimal storage,
89 including the pressure, permeability and thermal conductivity of the hydride
90 [20, 21]. However, there are too many complex elements like heat transfer,
91 metal hydride density should be taken into consideration in these models.

92 In the current stage of study for the embedded MH tank, the remaining
93 hydrogen mass is generally calculated by the integration of hydrogen flow rate
94 refueled in and released out. A gas flow sensor is well applied to measure the
95 gaseous hydrogen. However, during long-term operation, the measurement error
96 of flow sensor is accumulated along with the increased charging and discharging

97 cycle numbers. The expanding error of hydrogen flow leads to the decline of
98 estimation accuracy, it might resulting in an erroneous control strategy and an
99 irreversible damage on the properties of the MH hydrogen storage tank or other
100 related devices like fuel cell [22, 23]. Besides, the uncertain information of the
101 initial hydrogen concentration makes the SOC calculation inaccuracy. Thus, an
102 effective on-line SOC estimation method is necessary to measure and calibrate
103 the remaining hydrogen mass.

104 This work provides a new, simple, direct and effective method to evaluate
105 the hydrogen content stored in a MH hydrogen storage tank based on its char-
106 acterization and performance. The on-line SOC estimation process is developed
107 with physical analysis, statistical modeling and state classification, which is val-
108 idated by the database recorded on the real operation vehicles and proved to be
109 useful and efficient. In our study, a statistical model reflecting the relationship
110 between equilibrium pressure, temperature and SOC is proposed for describing
111 the performance of hydrogen storage and estimating the hydrogen capacity. The
112 operation condition and performance of the embedded hydrogen storage reactor
113 is more complicated with real operation requirements. So, the proposed statisti-
114 cal model might not satisfy to the precision requirement of the SOC estimation
115 mission at each time. In this study, the dynamic performance of the hydrogen
116 tank is analysed, from which a certain period is found to be available to apply
117 the statistical model for SOC estimation. Then, a state classifier is designed
118 to identify this state to realise the on-line SOC estimation of a MH hydrogen
119 storage tank embedded on fuel cell vehicle. Finally, the proposed on-line SOC
120 estimation process is validated by the database recorded on the real operation
121 vehicles in both charging and discharging situation.

122 **2. P-C-T based statistical model for SOC estimation**

123 In order to detect the features of the applied MH hydrogen storage tank on
124 the vehicle, a test bench in laboratory is built. On this test bench, a group of
125 validation database is collected using the similar way of D. Chabane did [24].

126 The experiments are carried out for both absorption and desorption reaction. In
127 absorption process, the initial conditions were set as the ambient temperature
128 and empty tank. The hydrogen flow rate is as low as 0.6kg/h for the purpose
129 of avoiding high kinetics and limiting temperature variations. The experiments
130 are carried out for both absorption and desorption reaction. In absorption
131 process, the initial conditions were set as the ambient temperature and empty
132 tank. During hydrogenation reaction, the exothermic absorption process causes
133 the temperature in the tank to raise, which also lead to the pressure increase.
134 By defining the threshold of temperature, the hydrogen mass flow filling into
135 the tank was controlled, which will be stopped when the temperature reached
136 the threshold. The system returns naturally to the ambient temperature after
137 energy convection and heat transfer. This process of charge will be repeated
138 several times until the tank is fully charged or completely empty. The desorption
139 process is in opposite direction. During the test, the remaining hydrogen mass
140 and the SOC of the MH tank are carefully controlled and calculated by the
141 hydrogen flow rate. The cumulative error is considered to be artificially avoided.
142 Thus, using a new tank in a strictly controlled experiment, the estimated SOC
143 is reliable to be considered as the calibrate reference.

144 From this database one can find that the data points of pressure at same
145 temperature are parts of a corresponding P-C-T isotherm of the tested MH
146 hydrogen storage tank. For each P-C-T isotherm of the tested MH tank, the
147 complete process of both hydrogenation and hydrogen extraction can be de-
148 scribed in three phases, including start to increase phase, slowly increase phase
149 and speedy increase phase. Moreover, all these P-C-T curves have the same
150 trend [25].

151 Correspondingly, the variation of the hydrogen mass absorbed by the MH
152 tank presents three stages, namely, slowly increase stage, speedy increase stage
153 and the stage of tend to be constant. During the first stage, the hydrogen
154 concentration is too low to active the hydrogenation reaction in a high speed.
155 Although the pressure increases rapidly, the absorption of hydrogen is slowly.
156 It comes to the second stage when the hydrogen to metal ratio reaches a certain

157 value, in which the reaction reaches to equilibrium state and advances smoothly.
 158 Thus, the hydrogen is absorbed in a high speed. When the MH tank is fully
 159 charged, the input hydrogen flow leads to the raise of pressure since no more
 160 hydrogen can be stored in the MH crystal. This feature of hydrogen mass
 161 variation is similar to the probability distribution function. Under this situation,
 162 the relationship among mass of hydrogen absorbed, pressure and temperature
 163 is able to be identified through the least squares method and the hydrogen mass
 164 can be directly described by the following equation, which means the statistical
 165 model to describe the variation of the hydrogen mass as a function of pressure
 166 P can be expressed as:

$$Mass = k1 + \frac{k2}{1 + exp(k3 * P + k4)} \quad (3)$$

167 In this equation, $Mass$ represents the hydrogen mass stored by the MH tank
 168 and P is the tank pressure. $k1$, $k2$, $k3$ and $k4$ are the coefficients reflecting
 169 the influence of temperature and durability on hydrogenation reaction. $k1$ cor-
 170 responds to the initial condition of the MH tank, ideally at the beginning of
 171 charging process, the tank is empty and $k1$ is zero. $k2$ corresponds to the hy-
 172 drogen storage capacity of the MH tank, namely, the hydrogen mass stored in
 173 a fully charged tank. The coefficients $k3$ and $k4$ are effected by temperature T
 174 and correspond to the equilibrium pressure in the tank, which will determine
 175 the shape of P-C-T isotherms.

176 In practical application of a MH hydrogen storage tank, the performance
 177 is also influenced by the state of health and the operation temperature. After
 178 larger number of charging and discharging cycles, the MH tank suffers from
 179 degradation so that the hydrogen storage capacity declines. Besides, the MH
 180 tank can not be completely discharged after degradation. Thus, the coefficient
 181 $k1 = mass_{ini}(n)$, which varies along with cycle number n . The capacity not
 182 only depends on the number of cycles n determined by the effect of ageing,
 183 but also corresponds to temperature. So, the coefficient $k2$ can be expressed
 184 as $mass(n, T)$. At the end of a charging process, the whole mass of hydrogen

185 stored in the MH tank $mass_{end}$ can be calculated by $k1 + k2$. In one cycle, the
 186 behaviour is determined by temperature. Therefore, the coefficients $k3 = f_1(T)$
 187 and $k4 = f_2(T)$ are the functions of temperature.

188 The SOC of MH tank at each moment i is the percentage of the available
 189 hydrogen mass stored in the tank to the total amount, which can be expressed
 190 as following equation:

$$SOC(i) = \frac{Mass(i) - mass_{ini}}{mass_{end}} * 100\% \quad (4)$$

191 where $Mass(i)$ corresponds to the mass of hydrogen extracted from the MH
 192 tank at this sampling time, $mass_{ini}$ represents the hydrogen mass rest in the
 193 crystal which can not be released under normal operation condition and $mass_{end}$
 194 is the hydrogen mass in a full tank.

Based on Eq. 3, the SOC model of a MH tank can be also expressed as
 follows:

$$SOC(i) = \frac{1}{1 + exp(f_1(T) * P + f_2(T))} * 100\% \quad (5)$$

195 It shows that the SOC of a MH tank is possible to be reflected by the pressure
 196 and temperature, no matter of the ageing degree. Thus, through measuring the
 197 performed state of a MH tank during charging or discharging process, its SOC
 198 can be estimated.

199 **3. On-line SOC estimation with a state classifier**

200 *3.1. Framework of the process*

201 The SOC estimation using the model presented in Eq. 5 is only adapted
 202 to a well-controlled experimental condition in the laboratory. The situation in
 203 practical application of the MH tank is more complicated, especially in trans-
 204 portation using. Taking the embedded MH hydrogen storage tank on a driving
 205 fuel cell vehicle as an example, the usage is under the requirement of driving
 206 mission. A whole continually charging or discharging process may not occur,
 207 namely, the discharging process might start from an uncertain SOC instead of

208 100%. At the beginning period, the gaseous hydrogen in the tank raised rapidly
 209 and the performance is mainly determined by the pressure difference between
 210 inside and outside of the tank. Therefore, the fault of SOC estimation cannot be
 211 avoided at this stage. When the dehydrogenating reaction is stable, the physical
 212 state of the tank is mainly depending on the equilibrium condition presented as
 213 P-C-T curves, which means that the pressure and temperature in this stage is
 214 determined by the hydrogen concentration. The SOC of the MH tank can be
 215 estimated with high accuracy using the proposed model in Eq. 5. Thus, the
 216 current state of reaction should be firstly recognized.

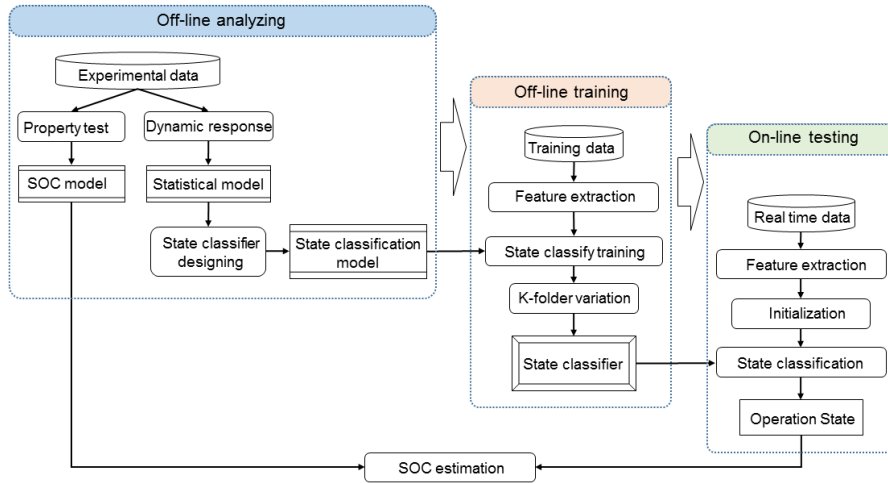


Fig. 1 - Framework of the on-line SOC estimation with a state classifier.

217 Fig. 1 gives the schematic of the framework for on-line SOC estimation. In
 218 this process, based on the property analysis of the reaction, a state classifier
 219 is firstly designed to identify the physical state of the MH reaction bed inside
 220 tank during operation. Then, after training the state classifier off-line using the
 221 historical database, it could characterize the real data recorded during opera-
 222 tion into its relating stage. This process can be realized on-line. Finally, the
 223 hydrogen concentration of a MH tank can be calculated rapidly to estimate the
 224 SOC on real time.

225 The off-line stage focuses on the historical database analysing and prepos-
226 sssing. In order to classify the state in a high speed, the optimal feature vectors
227 are required to be extracted from the database. The statistical characters reflect-
228 ing the properties including slope, kurtosis, entropy, *etc*, are of great potential as
229 the feature vectors for classify. Afterwards, the state classifier is trained by the
230 training set and adjusted by the testing set of feature vectors. Then, when the
231 well trained classifier comes to the on-line stage, the feature vectors extracted
232 from the real measured database is able to be classified. Therefore, the SOC
233 of the tank can be finally estimated. In this process, classifier is a model set
234 describing the characteristics and features of the database, which can be used
235 to identify the category of the unknown data, namely, map the unknown state
236 to a discrete classification set. The data-based classification method includes
237 fuzzy logic identification, neural network, Bayes classify, support vector ma-
238 chine (SVM) and so on. In this work, a joint multi-classifier is designed through
239 combining the Naive Bayes (NB) classifier and SVM classifier. The detailed
240 information will be presented below.

241 As discussed above, the hydrogenation reaction is stable in the second stage.
242 In addition, the hydrogen concentration can be achieved by the dynamic per-
243 formance of pressure and temperature. The stored hydrogen mass can therefore
244 be calculated by the proposed mathematical model, and the SOC of the MH
245 hydrogen storage tank can be estimated.

246 3.2. Design of the state classifier

247 As mentioned above, a joint multi-classifier constructed by a basic NB clas-
248 sifier and a multi SVM classifier are designed for state classification and identi-
249 fication of the MH tank reaction process.

250 NB classifier is developed based on the Bayes statistical theory, which can
251 be used to identify which category the observer belongs to. It has been widely
252 applied in many situations thanks to its high efficiency, high precision, and solid
253 theoretical foundation [26]. In practical applications, the application scope is
254 limited since it's hard to get the prior probability and the class conditional

255 probability density of each category. However, with appropriate independence
256 assumption, a smallest misclassification rate can still be achieved using NB clas-
257 sifier. SVM is a robust machine learning model that shows high accuracy with
258 different classification problems [27]. The accuracy of classification is guaranteed
259 for the high dimensional spaces and complex interaction characteristics. The
260 limitation of this method is that only two category classification problems can be
261 solved, which limits the application in complex state classification. Thus, a multi
262 SVM classifier is designed, which can decompose the multi-classification prob-
263 lem into several number of two-classification problems. Through decomposition
264 and reconstruction, two-classification problems can be solved respectively, and
265 the optimal results can then be determined. For the multi-classification prob-
266 lem with the category number of c , the SVM classifier is constructed between
267 each category. Therefore, the required SVM classifier number is $c(c-1)/2$. The
268 training samples of each SVM classifier are two related categories. The voting
269 method is used to determine the classification results that the category got the
270 maximum votes is the class that test sample belongs to. This kind of multi-
271 classifier has significant advantages. Since each SVM classifier only considers
272 two types of samples, the training process is simple to be achieved. Using the
273 majority voting method for making the final decision is easy to implement with
274 a high speed. Meanwhile, the classification accuracy is high. However, when
275 there are many categories to be distinguished, the number of SVM classifiers
276 increases sharply, which affects the training and testing speed, the accuracy
277 might be decreased as well.

278 Normally, the multi-classification model is integrated by the simple classi-
279 fiers in two ways that they connected in series or in parallel. In the series
280 multi-classifier, the classification information is transferred from the previous
281 simple classifier to the next one, which means the results of the previous simple
282 classifier and the other input information are combined as the input of the next
283 simple classifier. While in parallel multi-classifier, each simple classifier oper-
284 ates separately and the classification results are concluded in the end. Thus, its
285 speed of classification is significantly increased than that of series multi-classifier.

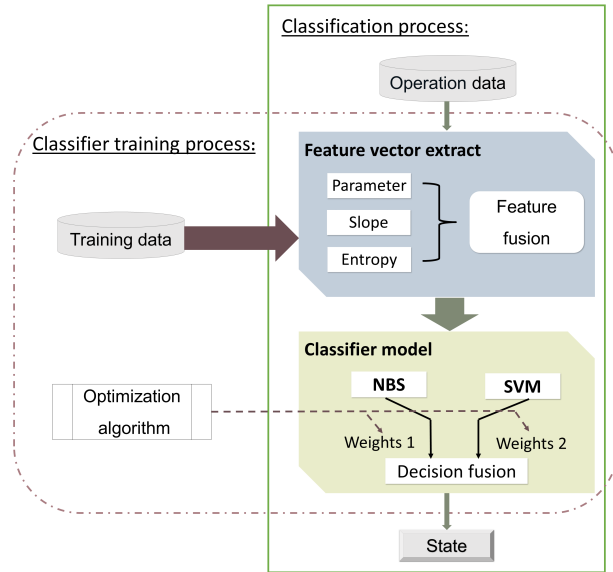


Fig. 2 - Flow chart of joint multi-classification.

286 What's more, the results of each simple classifier can be complementary. How-
 287 ever, if the simple classifiers and the combination rules are not properly selected,
 288 the results of the parallel multi-classifier may not rise but fall.

289 In this study, a joint multi-classifier in parallel structure is designed for
 290 the purpose of fully demonstrating the advantages while suppressing the weak-
 291 ness of each single basic classifier. Fig. 2 gives the flow chart of this joint
 292 multi-classifier. The multi SVM classifier and NB classifier are trained by the
 293 historical data separately, the results of each simple classifiers are afterwards
 294 learned and remembered. An optimization algorithm is used to search an opti-
 295 mal weight for the weighted summation of each simple classifier output result
 296 on the measurement layer. The final classification result is therefore be deter-
 297 mined. In this process, the combination weight is effected by the classification
 298 ability of simple classifiers and the state characteristics of the analyzed system.

299 **4. Experiments and validation**

300 *4.1. SOC estimation on test bench*

301 *4.1.1. Experiments on the test bench*

302 In our work, a test bench is built to validate the P-T-C based model for
303 SOC estimation in the laboratory. As presented in Fig. 3, two MH hydrogen
304 storage tanks are connected in parallel as the testing object. The properties
305 and reaction state are monitored and recorded. At the outlet of the tank, a gas
306 flow sensor is installed to record the hydrogen flow rate in and out the tank.
307 Besides, a pressure sensor is put at the tank gate to test the pressure inside the
308 tank. Two temperature sensors are attached at the surface of the MH tanks and
309 the measured results are considered as the reaction bed temperature. During
310 the reaction, the fan matrix, heater and circulation water operates together to
311 control the thermal condition. The fan matrix is used for heat transfer and heat
312 dissipation when the temperature is too high, while the heater is used to warm
313 the circulation water to provide more energy for reaction. Fig. 4 gives the photo
314 of the test bench.

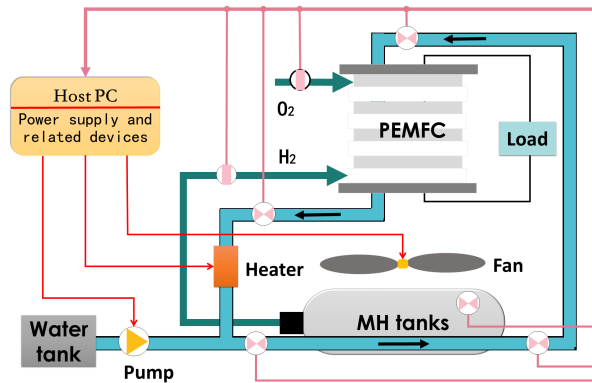


Fig. 3 - Schematic of the test bench.



Fig. 4 - Experimental setup.

315 During the test, the hydrogen is provided by the hydrogen tube in laboratory
 316 with the pressure of 7.5bar . The discharged hydrogen from the MH tank is
 317 released to the air circulation system. In other words, the hydrogen flow rate
 318 input and output of the MH tank is determined by the differential pressure.
 319 The experimental process is controlled by temperature. The temperature inside
 320 the test room is always kept as 19°C .

321 4.1.2. SOC estimation in absorption case

322 When charging the tanks, the generated heat raises the temperature of MH
 323 tanks. When the measured temperature reaches 26°C , the charging flow is
 324 stopped manually and the fan matrix is turned on to remove the heat. Until the
 325 MH tank temperature drop to 19°C , the charging process is restarted. This pro-
 326 cess repeats several times until the internal and external pressure is balanced,
 327 which means the MH tanks are fully charged. In contrary, the desorption reac-
 328 tion is an endothermic reaction that the MH tank temperature decreases during
 329 discharging. The circulation water is warmed by heater in order to raise the
 330 temperature of reaction bed. The temperature threshold is set as 22°C to 26°C .

331 From the database obtained on the test bench, the pressure and temperature
 332 under certain equilibrium state can be extracted. Then the SOC of the MH tank
 333 can be figured out through the statistical model presented in Eq. 5.

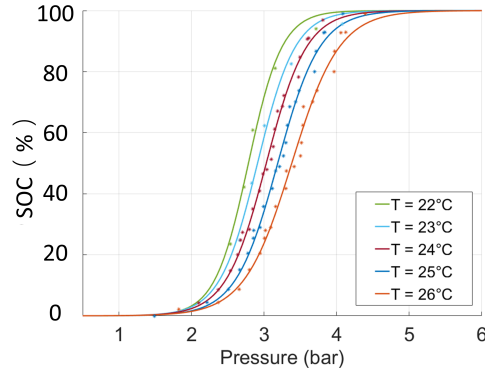


Fig. 5 - Parameter identification of the charging model.

334 Fig. 5 shows the identification results of the statistical model for SOC esti-
 335 mation of embedded MH tank during the whole process of absorption. As can be
 336 seen from each isotherm curve, the absorption process mainly occurred during
 337 the pressure varies from $2bar$ to $5bar$. When the hydrogen concentration is too
 338 low, hydrogen cannot be absorbed. The hydrogenation process will start after
 339 the concentration reaches a certain value. After the MH material in the tank
 340 was fully charged, the pressure rises steeply with the increased concentration
 341 of gaseous hydrogen. Table 2 presents the coefficients $f_1(T)$ and $f_2(T)$ used to
 342 draw these curves of the model in Fig. 5. The errors between the proposed
 343 model and the experimental data are acceptable that the maximum and the
 344 minimum value are 9.6% and 2.5%.

345 The hydrogen mass put into the MH tank is calculated by the measured
 346 hydrogen flow rate. Taking the calculated SOC as the calibration for evaluating
 347 the estimation results. From Fig. 5 one can see that the deviation of SOC
 348 estimation under different pressure are concentrated in the pressure zone of less
 349 than $2bar$, where the hydrogen concentration is not high enough and the main

350 absorption reaction is not carried out. Moreover, at the end period of charging
 351 process, the absorption speed is slow down and the gaseous hydrogen leads to
 352 the rapid increase of pressure. Thus, the SOC estimation based on the statistical
 353 model is not reliable enough when the pressure is high than $5bar$.

Table 2 - Identified parameters for absorption model.

T	$f_1(T)$	$f_2(T)$	Error
$22^\circ C$	-4.33	12.05	5.07%
$23^\circ C$	-3.85	11.19	5.81%
$24^\circ C$	-3.61	10.92	8.74%
$25^\circ C$	-3.44	10.98	8.33%
$26^\circ C$	-3.05	11.28	9.12%

In the SOC model, $f_1(T)$ and $f_2(T)$ reflect the influence of temperature on the equilibrium pressure, which will determine the shape of P-C-T curves of the reaction. The values of equilibrium pressure under each temperature could also be obtained by fitting the functions of $f_1(T)$ and $f_2(T)$. Through identifying how the coefficients variation with different temperatures, the function of $f_1(T)$ and $f_2(T)$ are identified as follows:

$$f_1(T) = 0.29 * T - 10.6 \quad (6)$$

$$f_2(T) = -0.368 * T + 19.1 \quad (7)$$

354 4.1.3. SOC estimation in desorption case

355 Similar to the absorption case, the data points of pressure under certain tem-
 356 perature during hydrogen desorption process can be extracted. Fig. 6 presents
 357 the results of the mathematical models representing the hydrogen concentra-
 358 tion stored in a MH hydrogen storage tank during desorption process, all these
 359 models are identified under different temperature while in one cycle.

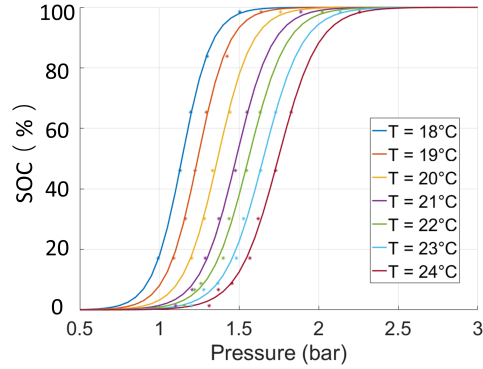


Fig. 6 - Parameter identification of the discharging model.

360 Obviously, the desorption process is normally carried out in a lower pressure
 361 zone than that of absorption. For the tested tank, the pressure is between
 362 1bar to 2bar. At the end period of discharging process, because of the small
 363 hydrogen concentration and low pressure, the desorption reaction cannot keep
 364 going automatically. Special measures are necessary to fully discharge a MH
 365 hydrogen storage tank like heating. However, during practical application the
 366 high temperature can not be achieved. The hydrogen retention in the tank will
 367 lead to the capacity degradation of an embedded MH tank after long time usage,
 368 which deserves special attention, which will be discussed later. The coefficients
 369 of the model for desorption process are presented in Table 3, in which the
 370 maximum error is as low as 2.47%. Similar to the charging process, the errors
 371 focus on the low pressure situation, namely, higher difficulty is inevitable for
 372 SOC estimation at low hydrogen concentration.

Table 3 - Identified parameters of SOC estimation model for desorption process.

T	$f_1(T)$	$f_2(T)$	Error
18°C	-10.74	12.26	1.14%
19°C	-10.14	12.58	2.73%
20°C	-9.29	12.69	4.55%
21°C	-8.72	12.92	9.56%
22°C	-8.49	13.23	9.36%
23°C	-8.22	13.58	9.35%
24°C	-800	13.97	9.21%

The function of $f_1(T)$ and $f_2(T)$ in *SOC* model during discharging process are identified as follows:

$$f_1(T) = 0.4782 * T - 19.1 \quad (8)$$

$$f_2(T) = 0.2422 * T + 7.9 \quad (9)$$

373 *4.2. On-line SOC estimation in real operation case*

374 *4.2.1. Validation procedure*

375 The online SOC estimation method, that combines the state classifier and
 376 SOC model, is verified on the database of the real fuel cell hybrid electrical
 377 vehicle (FCHEV) test[28]. In this project, ten FCHEVs are designed and op-
 378 erated. On these vehicles, two MH hydrogen storage tanks, same as the ones
 379 tested in laboratory, are connected in parallel to store hydrogen and supply the
 380 embedded fuel cell. The refuelling station provides gaseous hydrogen flow with
 381 constant pressure 10bar to charge the MH tank. During operation, the fuel cell
 382 system on the FCHEVs is used as the first power source to charge the batteries
 383 and then supply the vehicle load. Therefore, stable hydrogen flow is required

384 for constant fuel cell output power. The variation of the physical state during
 385 charging and discharging process of the embedded MH hydrogen storage tank
 386 are recorded separately.

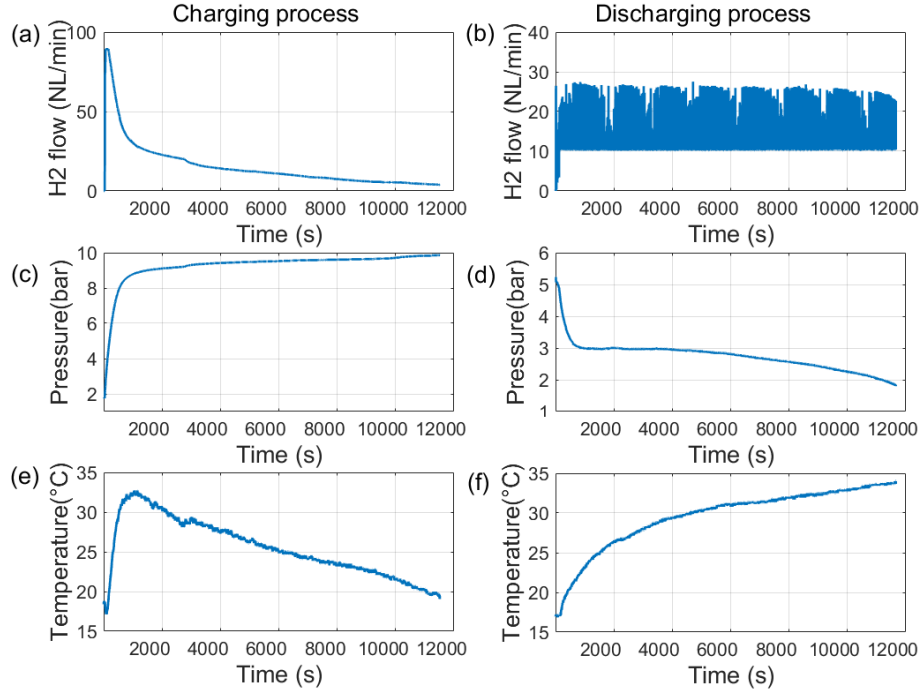


Fig. 7 - Physical state variation: (a)Hydrogen flow variation during charging process; (b)Hydrogen flow variation during discharging process; (c)Pressure variation during charging process; (b)Pressure variation during discharging process; (e)Temperature variation during charging process; (f)Temperature variation during discharging process.

387 Fig. 7 show the examples of the dynamic response of the MH hydrogen stor-
 388 age tanks. During charging process, the physical state variation presents two
 389 different stages. The first stage is dominated by the pressure difference so that
 390 the pressure and temperature increased rapidly with the high gaseous hydrogen
 391 flow imported to the tank. Then the hydrogen is absorbed by MH host material
 392 continuously, which leads to the pressure and temperature tend to constant.

393 In this stage, the temperature decreases due to the heat remove of the thermal
394 control system, which is used for accelerating the hydrogenation reaction. Com-
395 pared to the three hydrogenation reaction phases introduced above, these two
396 stages of practical application are also driven by external factors like pressure.
397 No matter of the initial hydrogen remaining in the tank, the performance of
398 the first stage shows the same tend. When the gaseous hydrogen concentra-
399 tion meets the hydrogenation conditions, the second stage starts, which will be
400 determined by the hydrogen to metal ratio.

401 The discharging process is separated into three stages. The hydrogen release
402 flow rate is controlled to be constant to meet the requirement of fuel cell con-
403 sumption. The thermal control system provide stable energy to heat the tank.
404 Similar to charging process, due to the pressure deference, the hydrogen pres-
405 sure drops quickly in the first stage. The temperature of MH tank raised rapidly
406 because of the low hydrogen generation reaction speed. When the hydrogen des-
407 orption reaction occurred stable and rapidly, the hydrogen generation speed is
408 high enough to satisfy the releasing requirement so that more heat is absorbed
409 for reaction. Thus, in the second stage, the pressure is maintained stable and
410 the temperature raised speed is slow down. The performance of third stage is
411 determined by the low SOC of MH tank. During the sorption procedure, the
412 equilibrium pressure drops at low hydrogen concentration, which also leads to
413 the decreased hydrogen generation speed. In order to hold the hydrogen releas-
414 ing speed, more heat absorption is needed. As a result, the pressure drops and
415 the rate of temperature raise decreases at the third stage.

416 The feature vectors selected for classification can reflect the characteristics
417 of each physical state in different stage. The time domain features of these
418 data based on statistical characteristics are typical for the performance since
419 the recorded data is time sampled. The energy density variation could also
420 present the characteristic of the data. Therefore, in this work, kurtosis feature
421 and entropy feature are also picked as classification feature vectors.

422 The optimal weight is searched during classifier training process using Grid
423 Search (GS) method. GS is an exhaustive search method that tests all the

424 set of the candidates' weights to find out the best performing one as the final
425 result. Thus, the optimal weight with highest classification precision is then
426 obtained. Since the number of categories is not too much, the disadvantage of
427 time consuming can be ignored.

428 Actually, both two single classifiers have a good consequent on the state clas-
429 sification of hydrogenation and dehydrogenating process, and the classification
430 accuracy rate of the tested databases have reached more than 70%. The NB
431 classifier has a simple structure, so the time required for classifier training and
432 state classification of each test data group is short. While the multiple SVM
433 classifier is composed of more than one single SVM classifiers, in which each
434 state category of the data is trained in pairs and takes a relatively long time.
435 However, the correct recognition rate of the test database by the joint multi-
436 classifiers is much higher than that of each single classifier, which has higher
437 application value. In the joint multi-classifier training, the GS algorithm needs
438 to perform multiple iterations when seeking the optimal weight, which leads to
439 a significant increase in training time compared to the single classifier. However,
440 the classification time for each set of test data is still short, which can meet the
441 time limit in practical applications.

442 *4.2.2. Method evaluation*

443 In order to evaluate the proposed on-line SOC estimation method, ten group
444 of real operation data are picked form charging and discharging database ran-
445 domly for validation. K-folds cross validation method is applied for testing the
446 classification accuracy of the designed joint multi-classifier. In each test pro-
447 cedure, 9 groups of data are set as the training set and the other one is set
448 for testing. After repeating the procedure for 10 times, the average value of
449 the mean square error of all the test procedure is regarded as the error of the
450 classifier.

451 For the SOC estimation of charging process, the combine weight of NB
452 classifier and SVM classifier are 0.5. Under this situation, the highest state
453 classification accuracy of 91.3% is achieved. While for discharging process, the

454 highest accuracy of state classification using joint multi-classifier is 83.2% with
455 the combine weight of 0.6 and 0.4, respectively for NB classifier and SVM clas-
456 sifier.

457 *4.2.3. On-line SOC estimation during vehicle charging*

458 As discussed above, the on-line SOC estimation during charging and dis-
459 charging process are quite difficult but important. Several groups of real opera-
460 tion data from Mobypost database are selected to validate the proposed on-line
461 SOC estimation algorithm. In the used database for charging process, the data
462 was recorded in refuelling station. On the vehicle management system, the hy-
463 drogen mass filling into the tank is calculated by the information from hydrogen
464 flow rate, which is used for calibrating the on-line estimation result.

465 Fig. 8(a) presents the state classification result during one charging process.
466 Obviously, the classification error is merely appears in transition of the first
467 stage to the second stage, which provides the possibility to estimate the SOC
468 using the statistical model in accuracy.

469 Fig. 8(b) gives the on-line SOC estimation result. Here, the source of the
470 picked data for validation is a charging process from completely released state
471 to fully charged state occurred on one FCHEV of Mobypost project. In this
472 project, the fuel cell mode stops when the SOC of the MH tank is lower than
473 10% for protecting fuel cell. As a result, the initial SOC is set as 10%. As
474 discussed above, the SOC estimation based on the proposed statistical model
475 is inaccuracy. Therefore, when the output of the on-line state classifier shows
476 the reaction is under the first stage, the SOC is calculated by the integration
477 with time of the hydrogen flow rate entered. Taking the calculated value on
478 the vehicle as calibration, the SOC estimation error is 0.2%. The fluctuation of
479 ambient temperature and the measurement deviation might be the main reason
480 causes the estimation error.

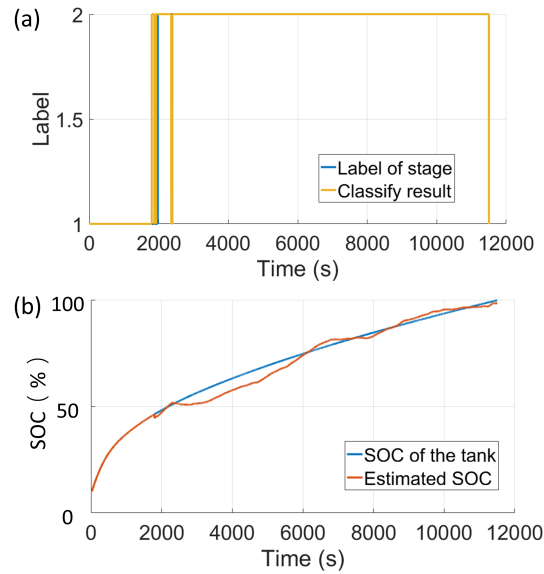


Fig. 8 - On-line test results for charging process. (a) On-line state classification result; (b) SOC estimation result.

481 *4.2.4. On-line SOC estimation during vehicle operation*

482 The discharging process is more complicated than charging, while it is more
 483 significant to estimate the SOC of embedded MH tank during vehicle operation.

484 The used database for validation was recorded in a continuously vehicle
 485 operation process, before that the hydrogen storage tank is fully charged at
 486 refuelling station. Therefore, the recorded data of remaining hydrogen mass is
 487 calculated by the released hydrogen flow rate.

488 Fig. 9(a) presents the on-line state classification result of the joint multi-
 489 classifier. It can be seen that the classification error is concentrated in the first
 490 stage and the third stage, while in the second stage, the performance of the
 491 classifier is excellent.

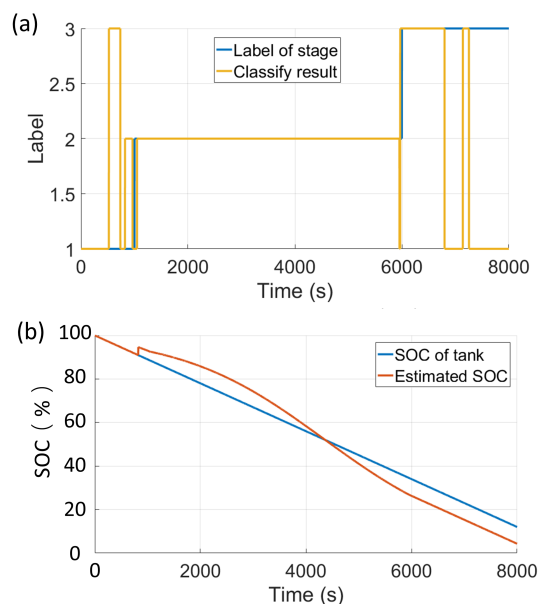


Fig. 9 - On-line test results for discharging process. (a)On-line state classification result; (b)SOC estimation result.

492 The classification result is used to estimate the SOC of the embedded MH
493 hydrogen storage tank. Based on the mathematical model proposed above,
494 the SOC of the tank can be calculated by the data point recognized as second
495 stage. Since the degradation of the MH hydrogen storage tank is not taken
496 into consideration, the hydrogen mass remained in the tank at the period of
497 recognized second stage can be estimated. Fig. 9(b) gives the estimation result,
498 in which the hydrogen mass in the first stage and third stage is calculated by
499 the recorded data of hydrogen flow rate. Compared to the value of hydrogen
500 mass in the tested database, the on-line SOC estimation results shows a great
501 agreement with the mean square error of 4.29%, which is acceptable. Besides,
502 the real operation data is recorded every second, and the testing time for one
503 group of data is less than $1 \times 10^{-4}s$. Thus, this on-line SOC estimation with
504 high accuracy and low time consumption is of high practical value.

505 **5. Conclusion**

506 This work focuses on the data based study of the MH hydrogen storage tank.
507 The studied database is collected from laboratory experiments and MobyPost
508 project separately, which are representative for reflecting the performance of
509 the hydrogenation reaction. The models designed in this work is based on
510 the statistical theory to characterize the performance of the main parameters
511 of reaction including pressure, temperature, hydrogen flow rate and hydrogen
512 mass. The P-C-T based SOC estimation method is proposed on the basis of
513 the main physical character of the reaction process. More data in a wide range
514 of distinct temperatures and long-term tests will be of great help to validate or
515 improve the proposed model. In addition, an effective on-line SOC estimation
516 method is proposed through designing a joint multi-classifier to recognize the
517 stage of reaction. Combined with the P-C-T based SOC model, the hydrogen
518 remaining in the tank can be estimated on real time. This method might be
519 not an accurate measurement of hydrogen sorption. However, it gives a solution
520 for on-board hydrogen storage SOC estimation, which can provide significant
521 information for the embedded energy management system.

522 **Acknowledgement**

523 The support from Chinese Scholarship Council (CSC), MobyPost project
524 funded under the Grant Agreement No.256834 by the European Union's sev-
525 enth Framework program (FP7/2007e2013) for the Fuel Cell and Hydrogen Joint
526 Technology Undertaking (<http://mobyPostproject.eu/>) and OenVHy project
527 funded by the Bourgogne-Franche comte region-France are gratefully acknowl-
528 edged.

529 **References**

- 530 [1] G. Dolf, B. Francisco, S. Deger, B. Morgan, D. W. Nicholas, G. Ricardo,
531 The role of renewable energy in the global energy transformation, Energy
532 Strategy Reviews 24 (2019) 38–50.

- 533 [2] S. Sharma, S. K. Ghoshal, Hydrogen the future transportation fuel: From
534 production to applications, *Renewable and Sustainable Energy Reviews* 43
535 (2015) 1151–1158.
- 536 [3] S. Mcdonagh, S. Ahmed, C. Desmond, J. D. Murphy, J. Yan, Hydrogen
537 from offshore wind: Investor perspective on the profitability of a hybrid
538 system including for curtailment, *Applied Energy* 265 (2020) 114732.
- 539 [4] Yang, Jun, Sudik, Andrea, Wolverton, Christopher, Siegel, J. Donald, High
540 capacity hydrogen storage materials: attributes for automotive applications
541 and techniques for materials discovery, *Chemical Society Reviews* 39 (2010)
542 656–675.
- 543 [5] P. R. Prabhukhot, M. M. Wagh, A. C. Gangal, A review on solid state
544 hydrogen storage material.
- 545 [6] M. Marinelli, M. Santarelli, Hydrogen storage alloys for stationary appli-
546 cations, *The Journal of Energy Storage* 32 (10) (2020) 101864.
- 547 [7] N. R. J. Hynes, R. Sankaranarayanan, P. S. Kannan, A. Khan,
548 H. Dzudzevic-Cancar, *Solid-state hydrides for hydrogen storage*, 2021.
- 549 [8] S. Koochi-Fayegh, M. A. Rosen, A review of energy storage types, applica-
550 tions and recent developments, *The Journal of Energy Storage* 27 (2020)
551 101047.
- 552 [9] T. Wei, K. L. Lim, Y. Tseng, S. Chan, A review on the characterization of
553 hydrogen in hydrogen storage materials, *Renewable and Sustainable Energy*
554 *Reviews* 79 (2017) 1122–1133.
- 555 [10] T. Blach, E. M. Gray, Sieverts apparatus and methodology for accurate
556 determination of hydrogen uptake by light-atom hosts, *Journal of Alloys*
557 *and Compounds* 446 (2007) 692–697.
- 558 [11] C. Webb, E. M. Gray, The effect of inaccurate volume calibrations on
559 hydrogen uptake measured by the sieverts method, *International Journal*
560 *of Hydrogen Energy* 39 (5) (2014) 2168–2174.

- 561 [12] C. Webb, E. M. Gray, Analysis of the uncertainties in gas uptake measure-
562 ments using the sieverts method, *International Journal of Hydrogen Energy*
563 39 (1) (2014) 366–375.
- 564 [13] F. A. Stevie, C. Zhou, M. Hopstaken, M. Saccomanno, Z. Zhang, A. Tu-
565 ransky, Sims measurement of hydrogen and deuterium detection limits in
566 silicon: Comparison of different sims instrumentation, *Journal of Vacuum*
567 *Science & Technology B, Nanotechnology and Microelectronics: Materials,*
568 *Processing, Measurement, and Phenomena* 34 (3) (2016) 03H103–1–3H103–
569 5.
- 570 [14] C. Wan, R. Denys, V. Yartys, In situ neutron powder diffraction study of
571 phase-structural transformations in the lamgmi battery anode alloy, *Journal*
572 *of Alloys and Compounds* 670 (2016) 210–216.
- 573 [15] I. Agency, Role of nuclear based techniques in development and characteri-
574 zation of materials for hydrogen storage and fuel cells, Role of nuclear based
575 techniques in development and characterization of materials for hydrogen
576 storage and fuel cells, 2012.
- 577 [16] L. Xi, Z. Qi, L. Haiyan, Y. Hongguang, L. Tao, L. Qian, Numerical anal-
578 ysis of the effects of particle radius and porosity on hydrogen absorption
579 performances in metal hydride tank - sciencedirect, *Applied Energy* 250
580 (2019) 1065–1072.
- 581 [17] S. Mohammadshahi, E. M. Gray, C. Webb, A review of mathematical mod-
582 elling of metal-hydride systems for hydrogen storage applications, *Interna-*
583 *tional Journal of Hydrogen Energy* 41 (5) (2016) 3470–3484.
- 584 [18] K. Minko, V. Artemov, G. Yan'kov, Numerical simulation of sorp-
585 tion/desorption processes in metal-hydride systems for hydrogen storage
586 and purification. part ii: verification of the mathematical model, *Interna-*
587 *tional Journal of Heat and Mass Transfer* 68 (2014) 693–702.

- 588 [19] A. Jemni, S. B. Nasrallah, Study of two-dimensional heat and mass transfer
589 during absorption in a metal-hydrogen reactor, *International Journal of*
590 *Hydrogen Energy* 20 (1) (1995) 43–52.
- 591 [20] A. Freni, F. Cipiti, G. Cacciola, Finite element-based simulation of a metal
592 hydride-based hydrogen storage tank, *International Journal of Hydrogen*
593 *Energy* 34 (20) (2009) 8574–8582.
- 594 [21] J. Nam, J. Ko, H. Ju, Three-dimensional modeling and simulation of hydro-
595 gen absorption in metal hydride hydrogen storage vessels, *Applied energy*
596 89 (1) (2012) 164–175.
- 597 [22] D. Arora, C. Bonnet, M. Mukherjee, S. Rael, F. Lapique, Direct hybridiza-
598 tion of pemfc and supercapacitors: Effect of excess hydrogen on a single
599 cell fuel cell durability and its feasibility on fuel cell stack, *Electrochimica*
600 *Acta* 310 (2019) 213–220.
- 601 [23] A. Ebadighajari, J. DeVaal, F. Golnaraghi, Optimal control of fuel over-
602 pressure in a polymer electrolyte membrane fuel cell with hydrogen transfer
603 leak during load change, *Journal of Power Sources* 340 (2017) 247–257.
- 604 [24] D. Chabane, F. Harel, A. Djerdir, D. Candusso, O. Elkedim, N. Fenineche,
605 A new method for the characterization of hydrides hydrogen tanks dedi-
606 cated to automotive applications, *international journal of hydrogen energy*
607 41 (27) (2016) 11682–11691.
- 608 [25] D. Zhu, Y. Ait-Amirat, A. N’Diaye, A. Djerdir, New dynamic modeling
609 of a real embedded metal hydride hydrogen storage system, *International*
610 *Journal of Hydrogen Energy* 44 (55) (2019) 29203–29211.
- 611 [26] Y.-C. Zhang, L. Sakhanenko, The naive bayes classifier for functional data,
612 *Statistics & Probability Letters* 152 (2019) 137–146.
- 613 [27] V. Vapnik, *The nature of statistical learning theory*, Springer science &
614 business media, 2013.
- 615 [28] <http://mobypost-project.eu>.